Monografías de la Real Academia de Ciencias de Zaragoza **34**, 27–50, (2010).

Mathematical modelling of pulverized coal furnaces

A. Bermúdez[1], J. L. Ferrín[1], A. Liñán[2] and L. Saavedra[1]

[1] Departamento de Matemática Aplicada, Universidad de Santiago de Compostela
15782 Santiago de Compostela, Spain

[2] E.T.S. Ingenieros Aeronáuticos, Universidad Politécnica de Madrid
Pl. Cardenal Cisneros 3, 28040 Madrid, Spain

1 Introduction

The goal of this paper is to show how mathematics and computational science can help to design not only the geometry but also the operation conditions of different parts of a pulverized coal power plant as the one shown in Figure 1.

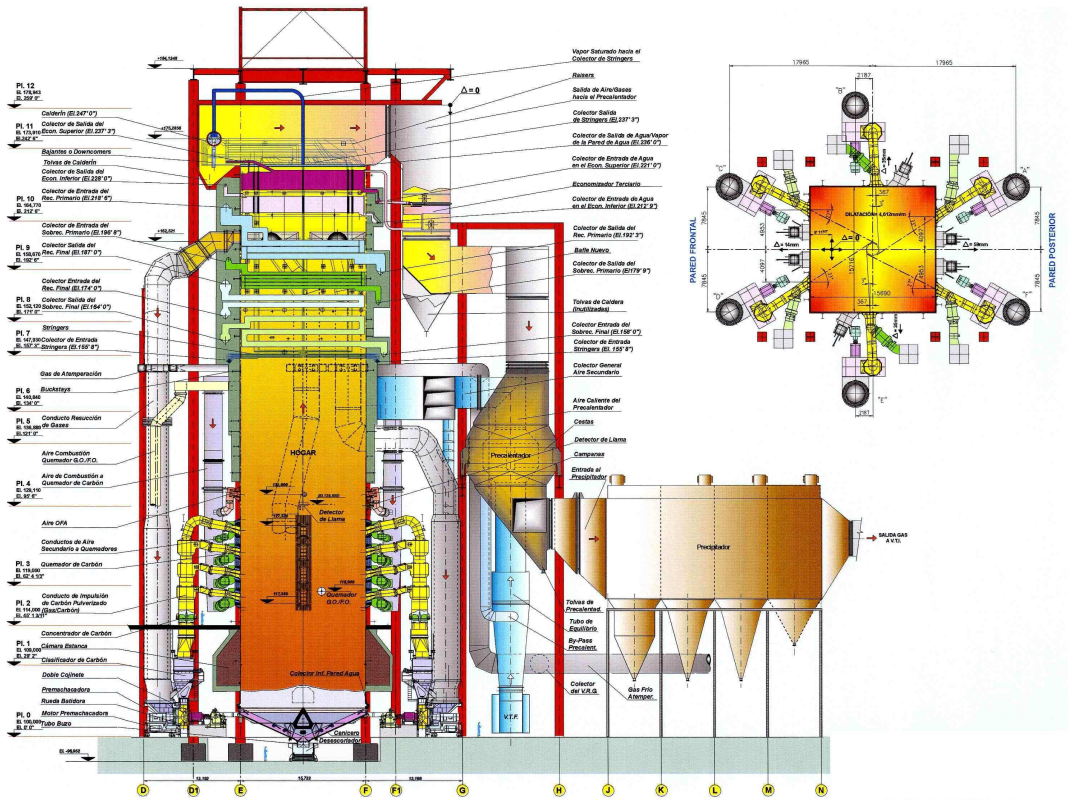

Figure 1.— Sketch of a coal fired power plant

In the last few years, the development of mathematical models and computational tools, including high performance computers and commercial computational fluid dynamics (CFD) packages, has allowed introducing the numerical simulation as an important tool to analyze the phenomena occurring in some different installations of a power plant.

For example, in Figure 2 the flow of secondary air dragging pulverized coal particles has been modelled, whereas in Figure 3 some numerical results corresponding to the simulation of erosion in the system of transport of ashes to silos are shown.

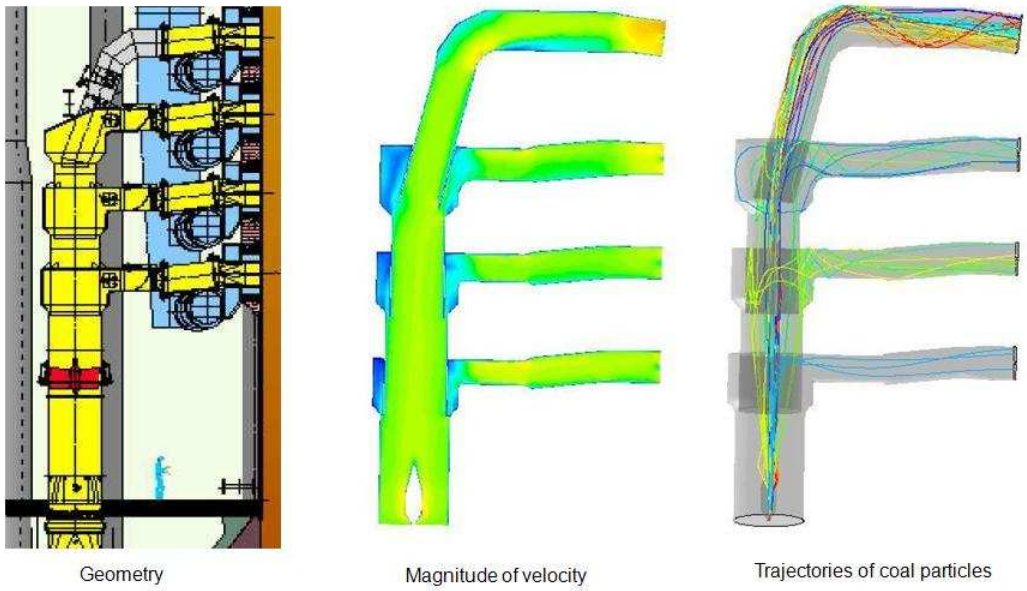

Figure 2.— System of coal input to the boiler

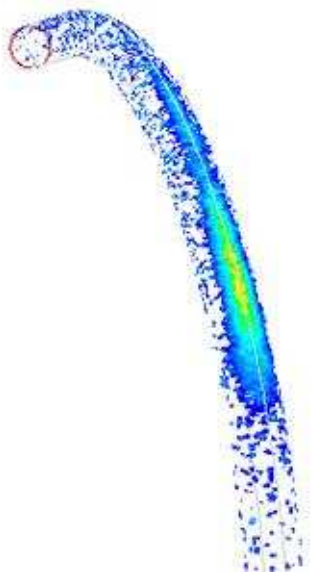

Figure 3.— Simulation of erosion

The main scope of this paper is to model and numerically solve the physico-chemical

processes occurring in the interior of the boiler, which is the part of the furnace where combustion of pulverized coal particles takes place (it can be seen at the center of Figure 1). CFD simulations can help to achieve a better performance of the installation in order to maximize the energetic efficiency, to minimize the NO_x formation, to control soiling phenomena or to assure a stable and sustainable ignition.

2 Mathematical modelling

In this section we present the mathematical model for a turbulent reactive two-phase flow taking place in the interior of the boiler. The two phases correspond to the gas mixture and to the solid coal particles. They will be described in an Eulerian-Lagrangian framework.

The gas phase model includes the conservation equations describing a steady, compressible, turbulent, radiant and reactive fluid. This fluid will be a mixture of O_2, CO_2, H_2O, $V_{(g)}$, CO, SO_2, H_2 and N_2.

The solid phase model must include the motion equation of a single particle and expressions for the sources from the solid phase to the gas one.

2.1 Gas phase model

We consider the standard equations for mass and momentum conservation, for the turbulence and for the thermal radiation, namely,

$$\nabla \cdot (\rho \mathbf{v}) = f^m, \tag{1}$$

$$\nabla \cdot (\rho \mathbf{v} \otimes \mathbf{v}) + \nabla p - \nabla \cdot \boldsymbol{\tau} = \rho \vec{g} + f^m \mathbf{v}_s, \tag{2}$$

$$\boldsymbol{\tau} = \mu_e \left(\nabla \mathbf{v} + \nabla \mathbf{v}^t \right) - \frac{2}{3} \mu_e (\nabla \cdot \mathbf{v}) \mathbf{I}, \tag{3}$$

$$\mathbf{v} \cdot \nabla k - \nabla \cdot \left[(\mu + \mu_t) \nabla k \right] = G_k - \rho \epsilon, \tag{4}$$

$$\mathbf{v} \cdot \nabla \epsilon - \nabla \cdot \left[\left(\mu + \frac{\mu_t}{1.3} \right) \nabla \epsilon \right] = 1.44 \frac{\epsilon}{k} G_k - 1.92 \frac{\epsilon^2}{k}, \tag{5}$$

$$\omega \cdot \nabla_x I + (a + \sigma_s) I - \frac{\sigma_s}{4\pi} \int_{S^2} \phi(\omega^*, \omega) I(x, \omega^*) d\omega^* = a I_b, \tag{6}$$

with $\mu_t = 0.09 \rho \frac{k^2}{\epsilon}$ and $G_k = \mu_t \| \nabla \mathbf{v} + (\nabla \mathbf{v})^t \|^2$.

Furthermore, we assume the low Mach number approximation, that is, we impose

$$\rho = \frac{\bar{p}}{RT} \tag{7}$$

where $\bar{p}$ denotes the average ambient pressure which is supposed to be constant in this state equation.

2.2 The combustion model

The combustion of coal particles, including devolatilization and char oxidation has been treated extensively in the literature (see, for example, [1] or [7]). The BFL combustion model introduced in Bermúdez *et al* [2] considers a simplified kinetic model consisting of the following physico-chemical process (reactions 1 to 5 within the porous particles and reactions 6 to 8 in the gas phase):

$$\underline{1} \qquad CO_2 + C_{(s)} \rightarrow 2\ CO \quad + (q_1)$$
$$\underline{2} \qquad \tfrac{1}{2}O_2 + C_{(s)} \rightarrow CO \quad + (q_2)$$
$$\underline{3} \qquad H_2O + C_{(s)} \rightarrow CO + H_2 \quad + (q_3)$$
$$\underline{4} \qquad V_{(s)} \rightarrow V_{(g)} \quad + (q_4)$$
$$\underline{5} \qquad H_2O_{(s)} \rightarrow H_2O_{(g)} \quad + (q_5)$$
$$\underline{6} \qquad CO + \tfrac{1}{2}\ O_2 \rightarrow CO_2 \quad + (q_6)$$
$$\underline{7} \qquad V_{(g)} + \nu_1\ O_2 \rightarrow \nu_2\ CO_2 + \nu_3\ H_2O + \nu_4\ SO_2 \quad + (q_7)$$
$$\underline{8} \qquad H_2 + \tfrac{1}{2}\ O_2 \rightarrow H_2O \quad + (q_8)$$

where indices s (respectively g) refers to the solid phase (respectively, to the gas phase). The q_i denotes the heat released in the i-th reaction per unit of gasified mass.

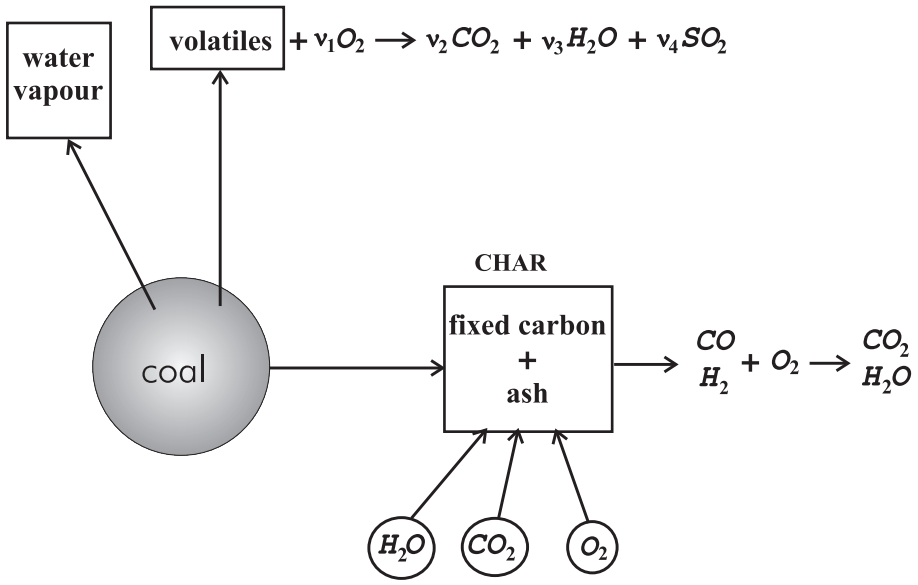

Figure 4.— Scheme of the combustion of a coal particle

For simplicity, in this paper we will consider the volatiles mixture represented by one single molecule,

$$V_{(g)} = C_{\kappa_1} H_{\kappa_2} O_{\kappa_3} S_{\kappa_4}, \tag{8}$$

of molecular mass $M_{\rm vol}$, where coefficients κ_1, κ_2, κ_3 and κ_4 are deduced from the ultimate analysis of the coal.

The stoichiometric coefficients ν_i are calculated in terms of the volatiles composition using the expressions: $\nu_1 = (2\kappa_1 + \kappa_2/2 + 2\kappa_4 - \kappa_3)/2$, $\nu_2 = \kappa_1$, $\nu_3 = \kappa_2/2$ and $\nu_4 = \kappa_4$.

For char oxidation we have considered a reduced mechanism including the three overall reactions 1, 2 and 3, of first order with respect to the local mean concentration of CO_2, O_2 and H_2O, measured by the product of the local gas density, ρ_g, times the mass fractions. We have considered the reactions to be of zero order with respect to the local char density, ρ_C. Obviously these three reaction rates must be equated to zero when the carbon of the particle is completely consumed, and therefore a Heaviside function is also included as a factor. More precisely, the local homogenized reaction rates per unit volume within the particle are modelled using global Arrhenius laws of the form

$$w_1 = B_1 e^{-E_1/\mathcal{R}T} \rho_g Y_{CO_2} H(\rho_C), \tag{9}$$

$$w_2 = B_2 e^{-E_2/\mathcal{R}T} \rho_g Y_{O_2} H(\rho_C), \tag{10}$$

$$w_3 = B_3 e^{-E_3/\mathcal{R}T} \rho_g Y_{H_2O} H(\rho_C), \tag{11}$$

where Y_{CO_2}, Y_{O_2} and Y_{H_2O} are the local mass fractions of CO_2, O_2 and H_2O in the gas filling the porous interstices and ρ_C is the density of carbon in the form of char. For the generation of volatiles and moisture evaporation we shall use the simple laws

$$w_4 = B_4 e^{-E_4/\mathcal{R}T} \rho_V, \tag{12}$$

$$w_5 = B_5 e^{-E_5/\mathcal{R}T} \rho_{H_2O}, \tag{13}$$

where ρ_V and ρ_{H_2O} are the local values within the coal particle of the density of volatiles and H_2O remaining in condensed form. The moisture generation is, for simplicity, here described with a kinetic model similar to the pyrolysis model of volatiles generation. We have chosen the rates of water vapour and volatiles generation to be of first order with respect to ρ_{H_2O} and ρ_V.

The fundamental assumption to obtain this model is the Burke-Schumann hypothesis. Therefore, the gas phase reactions 6 to 8 are supposed to be frozen or to occur with infinitely fast velocity in a gaseous thin diffusion flame that can be placed either inside the particle, or in the gas surrounding the particle or in the gas far from the particle. The type of combustion that will occur will depend on the temperature and local concentrations of oxygen, carbon monoxide, volatiles and H_2 in the gas environment; the model will decide in which situation the particle is.

The combustion model that we present in this paper consists of two coupled models: the gas phase model including the mass and energy conservation equations and the solid phase model. On the one hand the gas phase model determines the atmosphere in which particles are burnt and, on the other hand, the solid phase model provides mass and energy sources to the gas.

2.2.1 Gas phase Model

Let $\mathcal{L}_g$ be the differential operator defined by

$$\mathcal{L}_g(u) = \frac{\partial(\rho_g u)}{\partial t} + \nabla \cdot (\rho_g u \mathbf{v}_g) - \nabla \cdot (\rho_g \mathcal{D} \nabla u), \tag{14}$$

where $\mathcal{D}$ is a gas phase diffusion coefficient which, for simplicity, will be considered to be the same for all species and equal to the thermal diffusivity (Lewis number equal to one). Then, the conservation equations of the gaseous species are given by

$$\frac{\partial \rho_g}{\partial t} + \nabla \cdot (\rho_g \mathbf{v}_g) = f^{\mathrm{m}}, \tag{15}$$

$$\mathcal{L}_g(Y^g_{O_2}) = f^{\mathrm{m}}_{O_2} - \frac{4}{7} w_6 - \frac{32\nu_1}{M_{\mathrm{vol}}} w_7 - 8 w_8, \tag{16}$$

$$\mathcal{L}_g(Y^g_{CO_2}) = f^{\mathrm{m}}_{CO_2} + \frac{11}{7} w_6 + \frac{44\nu_2}{M_{\mathrm{vol}}} w_7, \tag{17}$$

$$\mathcal{L}_g(Y^g_{H_2O}) = f^{\mathrm{m}}_{H_2O} + \frac{18\nu_3}{M_{\mathrm{vol}}} w_7 + 9 w_8, \tag{18}$$

$$\mathcal{L}_g(Y^g_{SO_2}) = f^{\mathrm{m}}_{SO_2} + \frac{64\nu_4}{M_{\mathrm{vol}}} w_7, \tag{19}$$

$$\mathcal{L}_g(Y^g_{CO}) = f^{\mathrm{m}}_{CO} - w_6, \tag{20}$$

$$\mathcal{L}_g(Y^g_{V}) = f^{\mathrm{m}}_{V} - w_7, \tag{21}$$

$$\mathcal{L}_g(Y^g_{H_2}) = f^{\mathrm{m}}_{H_2} - w_8, \tag{22}$$

$$\mathcal{L}_g(h^g_T) = f^{\mathrm{e}} + q_6 w_6 + q_7 w_7 + q_8 w_8 - \nabla \cdot \mathbf{q}_{rg}, \tag{23}$$

where w_6, w_7 and w_8 denote, respectively, the mass consumption rates per unit volume of the volatiles, CO and H_2, due to the chemical reactions 6, 7 and 8, taking place in the gas phase; h^g_T is the gas phase specific thermal enthalpy, which we shall for simplicity write as $c_p T^g$ considering the gas phase specific heat at constant pressure, c_p, to be constant, and $\mathbf{q}_{rg}$ is the radiant heat flux vector.

The local homogenized reaction rates per unit volume within the particle could be modelled by using global Arrhenius laws of the form:

$$\begin{aligned} w_6 &= \rho_g^2 Y_{O_2}^{1/2} Y_{CO} Y_{H_2O}^{1/2} B_6 e^{-E_6/\mathcal{R}T}, \\ w_7 &= \rho_g^{1+\nu_1} Y_{O_2}^{\nu_1} Y_V B_7 e^{-E_7/\mathcal{R}T}, \\ w_8 &= \rho_g^{3/2} Y_{O_2}^{1/2} Y_{H_2} B_8 e^{-E_8/\mathcal{R}T}. \end{aligned}$$

Nevertheless, as we are considering the Burke-Schumann hypothesis of infinitely fast gas phase reactions, which implies the non coexistence of CO, V and H_2 with O_2, we do not need to provide expressions for the gas phase reaction rates. We can obtain equations

without the gas phase reaction terms considering the following conserved scalars of Shvab-Zeldovich type:

$$\beta_1^g = Y_{O_2}^g - \frac{4}{7}Y_{CO}^g - \frac{32\nu_1}{M_{\rm vol}}Y_V^g - 8Y_{H_2}^g, \tag{24}$$

$$\beta_2^g = Y_{CO_2}^g + \frac{11}{7}Y_{CO}^g + \frac{44\nu_2}{M_{\rm vol}}Y_V^g, \tag{25}$$

$$\beta_3^g = Y_{H_2O}^g + \frac{18\nu_3}{M_{\rm vol}}Y_V^g + 9Y_{H_2}^g, \tag{26}$$

$$\beta_4^g = Y_{SO_2}^g + \frac{64\nu_4}{M_{\rm vol}}Y_V^g, \tag{27}$$

$$H^g = h_T^g + q_6 Y_{CO}^g + q_7 Y_V^g + q_8 Y_{H_2}^g. \tag{28}$$

Then from (15)-(23) we have the equations

$$\mathcal{L}_g(\beta_1^g) = f_{O_2}^{\rm m} - \frac{4}{7}f_{CO}^{\rm m} - \frac{32\nu_1}{M_{\rm vol}}f_V^{\rm m} - 8f_{H_2}^{\rm m}, \tag{29}$$

$$\mathcal{L}_g(\beta_2^g) = f_{CO_2}^{\rm m} + \frac{11}{7}f_{CO}^{\rm m} + \frac{44\nu_2}{M_{\rm vol}}f_V^{\rm m}, \tag{30}$$

$$\mathcal{L}_g(\beta_3^g) = f_{H_2O}^{\rm m} + \frac{18\nu_3}{M_{\rm vol}}f_V^{\rm m} + 9f_{H_2}^{\rm m}, \tag{31}$$

$$\mathcal{L}_g(\beta_4^g) = f_{SO_2}^{\rm m} + \frac{64\nu_4}{M_{\rm vol}}f_V^{\rm m}, \tag{32}$$

$$\mathcal{L}_g(H^g) = f^{\rm e} + q_6 f_{CO}^{\rm m} + q_7 f_V^{\rm m} + q_8 f_{H_2}^{\rm m} - \nabla\cdot\mathbf{q}_{rg}. \tag{33}$$

Owing to the Burke-Schumann hypothesis we can determine two regions of the flow field: one region with oxygen, Ω_O, and another one without oxygen, Ω_F. The gas phase reactions 6 to 8 take place in a diffusion-controlled flame where the volatiles, CO and H_2 are burning with oxygen separating Ω_O from Ω_F. This surface is called Γ_F (see Figure 5 for details).

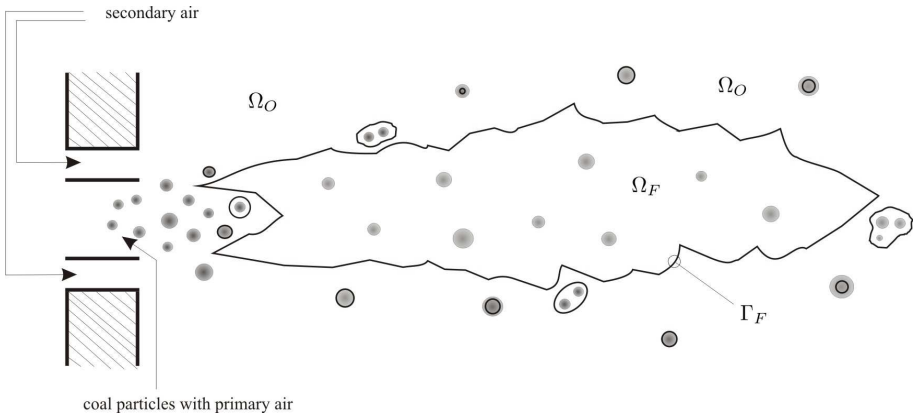

Figure 5.— Diffusion flame

Once we have solved (29), β_1^g will determine the regions of the domain and therefore the way to recover the mass fractions and the enthalpy from the Shvab-Zeldovich variables:

1. If $\beta_1^g > 0$ we are in the domain Ω_O, this implies that $Y_V^g = Y_{H_2}^g = Y_{CO} = 0$ and using (24)-(28) we obtain $Y_{O_2}^g = \beta_1^g$, $Y_{CO_2}^g = \beta_2^g$, $Y_{H_2O}^g = \beta_3^g$, $Y_{SO_2}^g = \beta_4^g$ and $h_T^g = H^g$.

2. If $\beta_1^g < 0$ we are in the domain Ω_F so $Y_{O_2}^g = 0$ and $w_6 = w_7 = w_8 = 0$. In this case to determine the mass fractions and the enthalpy we need to solve two additional equations of (21)-(23) without gas phase reaction terms.

2.2.2 Particle Gasification Model

The solid phase model is based on a Lagrangian computation of the temperature and density of each coal particle throughout its trajectory. We assume that the particles are spherical and its radius and its ash density remain constant during the combustion. So the model will be valid for particles with high content of ash.

The density of a coal particle is determined by:

$$\rho_p = \rho_{H_2O} + \rho_V + \rho_C + \rho_{ash}. \tag{34}$$

The evolution of ρ_{H_2O}, ρ_V and ρ_C, with radial coordinate r and time t, will be given by

$$\frac{\partial \rho_V}{\partial t} = -w_4, \qquad \frac{\partial \rho_{H_2O}}{\partial t} = -w_5, \qquad \frac{\partial \rho_C}{\partial t} = -w_C, \tag{35}$$

in terms of the mass rates, per unit volume and time, of generation of volatiles w_4, water vapour w_5 and char gasification w_C, given by equations (9)-(13).

To write the particle temperature equation we take into account that the heat conduction time across the particle is short compared with the diffusion time so we can consider the temperature spatially uniform. This temperature is given by the equation

$$\frac{4}{3}\pi a^3 \rho_p c_s \frac{dT_p}{dt} = 4\pi a^2 (q_p'' + q_r'') + \int_0^a \left(\sum_{i=1}^{8} q_i w_i \right) 4\pi r^2 dr, \tag{36}$$

where $4\pi a^2 q_p''$ and $4\pi a^2 q_r''$ are the heat flux by conduction and by radiation, respectively, which have the following expressions

$$q_p'' = k \frac{dT}{dr}_{|_{r=a^+}}, \quad q_r'' = \varepsilon_p \left(\frac{1}{4} \int_{S^2} I(x,\omega) d\omega - \sigma T_p^4 \right), \tag{37}$$

where $I(x,\omega)$ is the radiation intensity in the direction ω at the position of the particle, denoted by x, ε_p is the particle emissivity and S^2 is the unit sphere.

Due to the assumed uniformity of the temperature within the particle and the expressions (12) and (13), the rates of generation of water vapour and volatiles are spatially uniform and known functions of T_p and we can write the evolution with time of ρ_V and ρ_{H_2O} as

$$\frac{d\rho_V}{dt} = -B_4 e^{-E_4/\mathcal{R}T_p} \rho_V, \tag{38}$$

$$\frac{d\rho_{H_2O}}{dt} = -B_5 e^{-E_5/\mathcal{R}T_p} \rho_{H_2O}, \tag{39}$$

We cannot write a similar expression for the third equation in (35) because the dependence of ω_1, ω_2 and ω_3 on Y_{CO}, Y_{O_2} and Y_{H_2O}, which are not uniform within the particle. In fact, if we want to know the evolution of ρ_C, the values of Y_{CO}, Y_{O_2}, Y_{H_2O} have to be calculated using mass conservation equations for the gas phase within the pores of the particle for each given value of T_p and the mass fractions on the surface of the particle.

In order to simplify the treatment of the effects of the gasification char reactions 1, 2 and 3, Damköhler numbers have been defined for these reactions as

$$Da_i = \frac{a^2}{\mathcal{D}_e} B_i e^{-E_i/\mathcal{R}T_p}, \quad i = 1, 2, 3. \tag{40}$$

We consider that the activation energies of these heterogeneous reactions are large enough, so that Da_i are of order unity only a very short time. Damköhler numbers will determine the stage of char gasification:

- First stage ($Da_i \ll 1$, $i = 1, 2, 3$): kinetically-controlled reactions. Char gasification reactions can be considered frozen ($\omega_1 = \omega_2 = \omega_3 = 0$) and there is no production of CO or H_2 within the particle.

  So, to determine the particle density in the first stage, we only have to solve the equations (38) and (39). In this stage, the equation for the particle temperature (36) which can be simplified using that the gas phase reaction 7 is assume to be infinitely fast. Thus, if we compute the value β_1 at the particle surface

  $$\beta_1^s = Y_{O_2}^s - \frac{32\nu_1}{M_{vol}} Y_V^s, \tag{41}$$

  we have two different cases:

  - If $\beta_1^s < 0$ the reaction 7 takes place in a diffusion flame outside the particle and prevents the oxygen to reach the surface. In this case equation (36) becomes

    $$\frac{4}{3}\pi a^3 \rho_p c_s \frac{dT_p}{dt} = 4\pi a^2 (q_p'' + q_r'') + \int_0^a (q_4 w_4 + q_5 w_5)\, 4\pi r^2 dr, \tag{42}$$

  - If $\beta_1^s > 0$ the oxygen reaches the particle and reacts with the volatiles which cannot leave the particle. In this case the energy equation simplifies to

    $$\frac{4}{3}\pi a^3 \rho_p c_s \frac{dT_p}{dt} = 4\pi a^2 (q_p'' + q_r'') + \int_0^a (q_4 + q_7) w_4 + q_5 w_5 4\pi r^2 dr, \tag{43}$$

- Second stage ($Da_i \gg 1$, $i = 1, 2, 3$): diffusion-controlled reactions. Char gasification reactions are very fast and they occur in a diffusion flame at $r = r_c$ which implies that char and CO_2, O_2 and H_2O cannot coexist. This limit case leads to the "shrinking core model".

  The procedure which allows us to deduce the equations to be solved to determine ω_1, ω_2 and ω_3 in the second stage, as well as the expressions for the sources to the

gas phase, has been done in [2]. There are only two cases in which $\omega_2 \neq 0$, one in the limit case in which the gasification of char reactions are kinetically controlled and the other one when the oxygen reaches the particle core surface because of the small particle size based Damköhler numbers. Since we consider that this two cases are not relevant in our simulations, we will suppose, for simplicity of the implementation, that reaction 2 never takes place. Next, they are summarized taking into account that they are different depending on the domain in which the particle is and the position of the diffusion flame with respect to the particle:

1. Particle in Ω_F ($\beta_1^g < 0$). In this case we have to solve

$$\begin{aligned} \frac{11}{3}\frac{\lambda_1}{\lambda} &= \left\{ Y_{CO_2}^g + \frac{11}{3}\frac{\lambda_1}{\lambda} \right\} e^{\lambda \frac{\mathcal{D}}{\mathcal{D}_e}(1-a/r_c)-\lambda}, \\ \frac{3}{2}\frac{\lambda_3}{\lambda} - \frac{\lambda_5}{\lambda} &= \left\{ Y_{H_2O}^g + \frac{3}{2}\frac{\lambda_3}{\lambda} - \frac{\lambda_5}{\lambda} \right\} e^{\lambda \frac{\mathcal{D}}{\mathcal{D}_e}(1-a/r_c)-\lambda}, \end{aligned} \tag{44}$$

   where

$$\lambda_i = \frac{\dot{m}_i}{\rho_g a \mathcal{D}}, i = 1, 3, 4, 5, \tag{45}$$

   and $\mathcal{D}_e$ is the diffusion coefficient of the gas mixture inside the particle pores. The temperature equation is

$$\frac{4}{3}\pi a^3 \rho_p c_s \frac{dT_p}{dt} = 4\pi a^2 (q_p'' + q_r'') + 4\pi \rho_g a \mathcal{D}(q_1\lambda_1 + q_3\lambda_3 + q_4\lambda_4 + q_5\lambda_5), \tag{46}$$

   where

$$q_p'' = \frac{k}{ac_p}(h_T^g - h_T^s)\frac{\lambda}{e^\lambda - 1}. \tag{47}$$

2. Particle in Ω_O ($\beta_1^g > 0$) and $Y_{O_2}^s > 0$. The diffusion flame moves into the particle (i.e. $r_c < r_f \leq a$). The equations to solve are

$$\begin{aligned} & e^{\lambda \frac{\mathcal{D}}{\mathcal{D}_e}(a/r_f-1)+\lambda} = \varphi + 1, \\ & \frac{11}{3}\frac{\lambda_1}{\lambda} - \left[\frac{22}{3}\frac{\lambda_1}{\lambda} + \frac{11}{3}\frac{\lambda_3}{\lambda} + \frac{44\nu_2}{M_{\text{vol}}}\frac{\lambda_4}{\lambda} \right] e^{\lambda \frac{\mathcal{D}}{\mathcal{D}_e}(a/r_f - a/r_c)} \\ & \qquad = \left\{ Y_{CO_2}^g - \frac{11}{3}\left(\frac{\lambda_1}{\lambda} + \frac{\lambda_3}{\lambda} \right) - \frac{44\nu_2}{M_{\text{vol}}}\frac{\lambda_4}{\lambda} \right\} e^{\lambda \frac{\mathcal{D}}{\mathcal{D}_e}(1-a/r_c)-\lambda}, \\ & \frac{3}{2}\frac{\lambda_3}{\lambda} - \frac{\lambda_5}{\lambda} - \left(\frac{3}{2}\frac{\lambda_3}{\lambda} + \frac{18\nu_3}{M_{\text{vol}}}\frac{\lambda_4}{\lambda} \right) e^{\lambda \frac{\mathcal{D}}{\mathcal{D}_e}(a/r_f - a/r_c)} \\ & \qquad = \left\{ Y_{H_2O}^g - \frac{\lambda_5}{\lambda} - \frac{18\nu_3}{M_{\text{vol}}}\frac{\lambda_4}{\lambda} \right\} e^{\lambda \frac{\mathcal{D}}{\mathcal{D}_e}(1-a/r_c)-\lambda}, \end{aligned} \tag{48}$$

   with φ given by

$$\varphi = \frac{Y_{O_2}^g}{\frac{8}{3}\left(\frac{\lambda_1}{\lambda} + \frac{\lambda_3}{\lambda}\right) + \frac{32\nu_1}{M_{\text{vol}}}\frac{\lambda_4}{\lambda}}. \tag{49}$$

The temperature equation is

$$\begin{aligned}\frac{4}{3}\pi a^3\rho_p c_s\frac{dT_p}{dt} &= 4\pi a^2(q_p''+q_r'')+4\pi\rho_g a\mathcal{D}(q_1\lambda_1+q_3\lambda_3+q_4\lambda_4+q_5\lambda_5\\ &+ \frac{14}{3}q_6\lambda_1+\frac{7}{3}q_6\lambda_3+q_7\lambda_4+\frac{1}{6}q_8\lambda_3)\end{aligned} \tag{50}$$

where q_p'' is given by (47).

3. Particle in Ω_O ($\beta_1^g > 0$) and $Y_{O_2}^s = 0$. The diffusion flame is surrounding the particle (i.e. $r_f > a$). In this case we have to solve

$$\begin{aligned}\frac{11}{3}\frac{\lambda_1}{\lambda} &= \left\{Y_{CO_2}^g+\frac{11}{3}\frac{\lambda_1}{\lambda}+\left(\frac{22}{3}\frac{\lambda_1}{\lambda}+\frac{11}{3}\frac{\lambda_3}{\lambda}+\frac{44\nu_2}{M_{\text{vol}}}\frac{\lambda_4}{\lambda}\right)\varphi\right\}e^{\lambda\frac{\mathcal{D}}{\mathcal{D}_e}(1-a/r_c)-\lambda},\\ \frac{3}{2}\frac{\lambda_3}{\lambda}-\frac{\lambda_5}{\lambda} &= \left\{Y_{H_2O}^g+\frac{3}{2}\frac{\lambda_3}{\lambda}-\frac{\lambda_5}{\lambda}+\left(\frac{3}{2}\frac{\lambda_3}{\lambda}+\frac{18\nu_3}{M_{\text{vol}}}\frac{\lambda_4}{\lambda}\right)\varphi\right\}e^{\lambda\frac{\mathcal{D}}{\mathcal{D}_e}(1-a/r_c)-\lambda}.\end{aligned} \tag{51}$$

The temperature equation is

$$\begin{aligned}\frac{4}{3}\pi a^3\rho_p c_s\frac{dT_p}{dt} &= 4\pi a^2(q_p''+q_r'')+4\pi\rho_g a\mathcal{D}(q_1\lambda_1+q_3\lambda_3+q_4\lambda_4+q_5\lambda_5\\ &+ \frac{14}{3}q_6\lambda_1+\frac{7}{3}q_6\lambda_3+q_7\lambda_4+\frac{1}{6}q_8\lambda_3)\end{aligned} \tag{52}$$

where

$$q_p'' = \frac{k}{ac_p}\frac{\lambda}{e^\lambda-1}\left\{h_T^g-h_T^s+\left[q_6\left(\frac{14}{3}\frac{\lambda_1}{\lambda}+\frac{7}{3}\frac{\lambda_3}{\lambda}\right)+q_7\frac{\lambda_4}{\lambda}+q_8\frac{1}{6}\frac{\lambda_3}{\lambda}\right]\varphi\right\}. \tag{53}$$

In all the three cases, the position of the shrinking core is given by

$$\frac{\rho_C^0}{\rho_g a\mathcal{D}}r_c^2\frac{dr_c}{dt} = -(\lambda_1+\lambda_3). \tag{54}$$

2.2.3 Sources to the gas phase

The purpose of solving the solid phase model is to obtain the sources of mass and energy to the gas phase from coal particles gasification. Once we know this sources we can solve equations (29)-(33) and obtain the temperature and composition of the gas mixture.

The expressions for the sources of mass of each of the species due to one single particle are:

1. In Ω_F ($Y^g_{O_2} = 0$):

$$F^m_{O_2} = F^m_{SO_2} = 0, \tag{55}$$

$$F^m_{CO_2} = \frac{4\pi ak}{c_p}\left(-\frac{11}{3}\lambda_1\right), \tag{56}$$

$$F^m_{H_2O} = \frac{4\pi ak}{c_p}\left(\lambda_5 - \frac{3}{2}\lambda_3\right), \tag{57}$$

$$F^m_{CO} = \frac{4\pi ak}{c_p}\left(\frac{14}{3}\lambda_1 + \frac{7}{3}\lambda_3\right), \tag{58}$$

$$F^m_{V} = \frac{4\pi ak}{c_p}\lambda_4, \tag{59}$$

$$F^m_{H_2} = \frac{4\pi ak}{c_p}\frac{1}{6}\lambda_3. \tag{60}$$

2. In Ω_O ($Y^g_{O_2} > 0$):

$$F^m_{O_2} = \frac{4\pi ak}{c_p}\left(-\frac{8}{3}(\lambda_1 + \lambda_3) - \frac{32\nu_1}{M_{\text{vol}}}\lambda_4\right), \tag{61}$$

$$F^m_{CO_2} = \frac{4\pi ak}{c_p}\left(\frac{11}{3}(\lambda_1 + \lambda_3) + \frac{44\nu_2}{M_{\text{vol}}}\lambda_4\right), \tag{62}$$

$$F^m_{H_2O} = \frac{4\pi ak}{c_p}\left(\lambda_5 + \frac{18\nu_3}{M_{\text{vol}}}\lambda_4\right), \tag{63}$$

$$F^m_{SO_2} = \frac{4\pi ak}{c_p}\frac{64\nu_4}{M_{\text{vol}}}\lambda_4, \tag{64}$$

$$F^m_{CO} = F^m_{V} = F^m_{H_2} = 0. \tag{65}$$

Both in Ω_O and in Ω_F the total source of mass is

$$F^m = \frac{4\pi ak}{c_p}\lambda \tag{66}$$

and the source of energy is

$$F^e = 4\pi ak\left\{(\frac{c_s}{c_p}T_p - T_g)\frac{\lambda}{e^\lambda - 1} + (1-\vartheta)\left[\frac{q_6}{c_p}\left(\frac{14}{3}\lambda_1 + \frac{7}{3}\lambda_3\right) + \frac{q_7}{c_p}\lambda_4 + \frac{q_8}{c_p}\frac{1}{6}\lambda_3\right]\right\} - c_s T_p\frac{dm_p}{dt}, \tag{67}$$

where

$$\vartheta = \begin{cases} 1 & \text{when } \beta^s_1 > 0 \text{ (flame inside the particle) or} \\ & \beta^g < 0 \text{ (there is no oxygen in the vicinity),} \\ \dfrac{\varphi}{e^\lambda - 1} & \text{when } \beta^g_1 > 0 \text{ and } \beta^s_1 < 0 \text{ (flame outside the particle),} \end{cases}$$

The homogenized sources in the gas phase per unit volume and time, at point x, are computed adding the contributions of each single particle that at some instant t is at point x by the expression

$$f^\alpha(\mathbf{x}) = \sum_{j=1}^{N_e}\sum_{i=1}^{N_p}\tilde{q}_j\frac{p_{ij}}{100}\int_0^{t^{ij}_f} F^\alpha_{ij}(t)\delta(\mathbf{x} - \mathbf{x}^{ij}_p(t))dt \tag{68}$$

where $F_{ij}^{\alpha}(t)$ is the source of mass or energy of one particle of type i introduced through inlet j, at instant t, $\mathbf{x}_p^{ij}(t)$ is the position occupied by this particle at instant t, $\delta(x)$ is the Dirac measure at point 0, t_f^{ij} is the time needed for the particle to be completely burned or to leave the furnace, $\tilde{q}_j$ is the mass flow of coal through the inlet j, p_{ij} is the percentage of particles of the type i through inlet j, and N_e and N_p are the number of inlets and types of particles, respectively.

2.3 Particle Motion Model

To solve the solid phase model we need to follow each single particle along the domain. We will suppose that the forces affecting the particle motion are only the drag force and the gravity. We obtain the particle velocity by solving the ordinary differential equation:

$$\frac{d\mathbf{v}_p}{dt} = F_A\left(\mathbf{v}_g - \mathbf{v}_p\right) + \mathbf{g}, \tag{69}$$

$$\mathbf{v}_p(0) = \mathbf{v}_{p0}, \tag{70}$$

where F_A is the drag force per mass unit which can be written as

$$F_A = \frac{3}{16}\frac{\mu}{\rho_p a^2} C_D Re. \tag{71}$$

Here $\mathbf{v}_g$ is the gas mixture velocity, $\mathbf{v}_p$ the particle velocity, μ the gas viscosity, Re is the Reynolds number relative to the particle, namely,

$$Re = \rho_g \mid \mathbf{v}_g - \mathbf{v}_p \mid \frac{2a}{\mu}, \tag{72}$$

and C_D is the drag coefficient which can be deduced from

$$C_D = \begin{cases} \frac{1+0.15Re^{0.687}}{Re/24} & \text{if } Re \leq 1000, \\ 0.44 & \text{in other case.} \end{cases}$$

2.3.1 Stochastic Particle Dispersion Modelling

In the particle motion model that we propose, coal particles only respond to the mean fluid velocity. This is correct if the flow is laminar but if we consider a turbulent flow we must take into account the effect of a random fluctuating velocity. For this purpose we have coupled the particle motion model with a discrete random walk model. This type of models specify the velocity as the sum of the mean fluid velocity and a Gaussian distributed random velocity fluctuation with zero mean and a variance related to the turbulent velocity scale computed from the turbulence model used. The random value of the velocity is kept constant over an interval of time given by the characteristic lifetime of the eddies, as made by [8].

Since we use the $k-\epsilon$ turbulence model, the instantaneous fluid velocity is calculated as

$$\mathbf{v}_g = \bar{\mathbf{v}}_g + \left(\xi_1 \sqrt{\frac{2k}{3}}, \xi_2 \sqrt{\frac{2k}{3}}, \xi_3 \sqrt{\frac{2k}{3}} \right), \tag{73}$$

where $\xi_i, i = 1, 2, 3$, are normally distributed random numbers. The eddy time scale that we consider is

$$\tau_e = -0.15 \frac{k}{\epsilon} log(r), \tag{74}$$

where r is a uniform random number between 0 and 1. The particle eddy crossing time is given by

$$\tau_c = -\tau \log \left(1 - \frac{L_e}{\tau \|\mathbf{v}_g - \mathbf{v}_p\|} \right), \tag{75}$$

where $\tau = 1/F_A$ is the particle relaxation time and

$$L_e = 0.09 \frac{k^{1.5}}{\epsilon} \tag{76}$$

is the eddy length scale.

As many random walk models, this model produces reasonable behavior in flows with homogeneous turbulence. The suitability of many random walk models and others particle dispersion models is analyzed in [6] or in [9] to include the effect of anisotropy.

We compute the trajectory, the density, the temperature and the sources to the gas phase for a sufficient number of representative particles ("number of tries") with different sizes, dropped from each cell of each inlet (as seen in Figure 6).

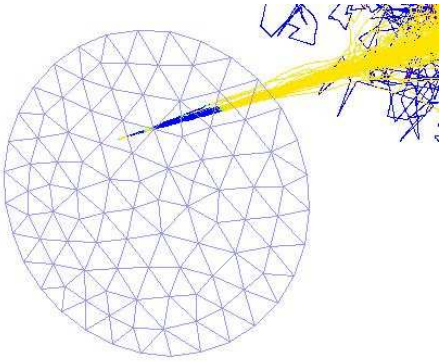

Figure 6.— Trajectories of particles from a single cell

3 Algorithm and numerical methods

In order to numerically solve the different equations of the coupled two-phases problem we implement a segregated procedure, leading to the algorithm shown in Figure 7.

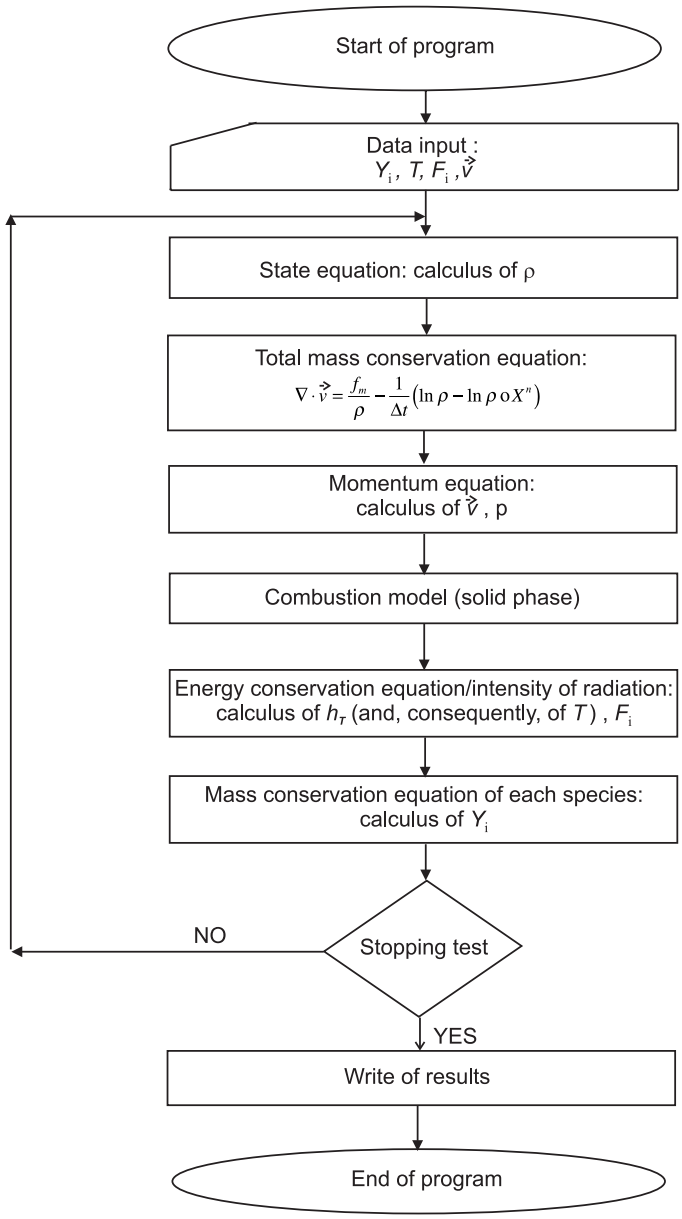

Figure 7.— Global algorithm

In the next subsections we describe the numerical methods used to solve the equations of each problem in the sequential algorithm of Figure 7.

3.1 Momentum conservation equations

For solving the steady-state Navier-Stokes equations we use a P_1-bubble/P_1 mixed finite element combined with the method of characteristics and proceed to the elimination of bubbles prior to the assembly by static condensation. Thus, we have to solve the

following boundary-value problem:

$$\begin{cases} \rho\dfrac{3\mathbf{v}-4\mathbf{v}\circ X^{\Delta t}+\mathbf{v}\circ X^{2\Delta t}}{2\Delta t}-\nabla\cdot\boldsymbol{\tau}+\nabla p=f \quad \text{in } \Omega \\ \nabla\cdot\mathbf{v}=\dfrac{f_m}{\rho}-\dfrac{1}{2\Delta t}(3\ln\rho-4\ln\rho\circ X^{\Delta t}+\ln\rho\circ X^{2\Delta t}) \quad \text{in } \Omega \\ \mathbf{v}=\mathbf{v}_e \quad \text{on } \Gamma_e \\ \mathbf{v}=0 \quad \text{on } \Gamma_p \\ \boldsymbol{\tau}\vec{n}-p'\vec{n}=0 \quad \text{on } \Gamma_s \end{cases}$$

where $X^{\Delta t}(x)=\chi(x,\Delta t;0)$ and $X^{2\Delta t}(x)=\chi(x,2\Delta t;0)$.

For that, we propose the following algorithm:

Step 0. Input $\mathbf{v}^0$ y p^0

Step 1. Given $\mathbf{v}^0$ and p^0 , $\mathbf{v}^1$ and p^1 are the solution of the system:

$$\begin{cases} \displaystyle\int_\Omega \frac{1}{\Delta t}\rho\mathbf{v}^1\vec{z}dx+\int_\Omega \mu_e(\nabla\mathbf{v}^1+(\nabla\mathbf{v}^1)^T):\nabla\vec{z}dx-\int_\Omega \tilde{p}^1\nabla\cdot\vec{z}dx=\int_\Omega f^1\vec{z}dx+ \\ \qquad\qquad +\displaystyle\int_\Omega \frac{1}{\Delta t}\rho\mathbf{v}^0\circ X^0\vec{z}dx \\ \displaystyle\int_\Omega \nabla\cdot\mathbf{v}^1qdx=\int_\Omega g\ qdx \\ \mathbf{v}^1=\mathbf{v}_e \quad \text{on } \Gamma_e \\ \mathbf{v}^1=0 \quad \text{on } \Gamma_p \end{cases}$$

with

$$g=\frac{f_m}{\rho}-\frac{1}{\Delta t}(\ln\rho-\ln\rho\circ X^0),$$

$$\tilde{p}=p+\frac{2}{3}\mu_e g.$$

Step n ($n\geq 1$). Given $\mathbf{v}^{n-1}$, $\mathbf{v}^n$, p^{n-1} and p^n, $\mathbf{v}^{n+1}$ and p^{n+1} are the solution of the system:

$$\begin{cases} \displaystyle\int_\Omega \frac{3}{2\Delta t}\rho\mathbf{v}^{n+1}\vec{z}dx+\int_\Omega \mu_e(\nabla\mathbf{v}^{n+1}+(\nabla\mathbf{v}^{n+1})^T):\nabla\vec{z}dx-\int_\Omega \tilde{p}^{n+1}\nabla\cdot\vec{z}dx=\int_\Omega f^{n+1}\vec{z}dx+ \\ \qquad\qquad +\displaystyle\int_\Omega \frac{2}{\Delta t}\rho\mathbf{v}^n\circ X^n\vec{z}dx-\int_\Omega \frac{1}{2\Delta t}\rho\mathbf{v}^{n-1}\circ X^{n-1}\vec{z}dx \\ \displaystyle\int_\Omega \nabla\cdot\mathbf{v}^{n+1}qdx=\int_\Omega g\ qdx \\ \mathbf{v}^{n+1}=\mathbf{v}_e \quad \text{on } \Gamma_e \\ \mathbf{v}^{n+1}=0 \quad \text{on } \Gamma_p \end{cases}$$

with

$$g = \frac{f_m}{\rho} - \frac{1}{2\Delta t}(3\ln\rho - 4\ln\rho\circ X^n + 3\ln\rho\circ X^{n-1}),$$

$$\tilde{p} = p + \frac{2}{3}\mu_e g.$$

Discretizing and eliminating the bubbles for all steps, this leads to a linear system with the following structure:

$$\begin{pmatrix} A & 0 & 0 & B^{(1)^T} \\ 0 & A & 0 & B^{(2)^T} \\ 0 & 0 & A & B^{(3)^T} \\ B^{(1)} & B^{(2)} & B^{(3)} & C \end{pmatrix} \begin{pmatrix} v_1 \\ v_2 \\ v_3 \\ \tilde{p} \end{pmatrix} = \begin{pmatrix} S_1^{(1)} \\ S_1^{(2)} \\ S_1^{(3)} \\ S_2 \end{pmatrix}$$

3.2 Radiation

For the equation of the intensity of radiation we use a six-flux method for the semidiscretization in ω and choose between a finite element method and a finite difference method (the latter is only valid for a structured mesh), for spatial discretization.

The equations to be solved are

$$\begin{cases} \omega\cdot\nabla_x I + (a+\sigma_s)I - \dfrac{\sigma_s}{4\pi}\displaystyle\int_{S^2}\phi(\omega^*,\omega)I(x,\omega^*)d\omega^* = aI_b \quad \text{in } \Omega, \\ I(x) = \dfrac{1-\varepsilon_w}{\pi\varepsilon_w}\ \vec{q_r}\cdot\vec{n} + \dfrac{\sigma T_w^4}{\pi} \quad \text{on } \Gamma. \end{cases}$$

3.2.1 Six-flux method

Let $\hat{I}(x,\cdot) \in W :=< w_1,\ldots,w_6 >$ and

$$\begin{aligned} I_1^+(x) &= \hat{I}(x,\omega^1) \qquad I_1^-(x) = \hat{I}(x,\omega^2) \\ I_2^+(x) &= \hat{I}(x,\omega^3) \qquad I_2^-(x) = \hat{I}(x,\omega^4) \\ I_3^+(x) &= \hat{I}(x,\omega^5) \qquad I_3^-(x) = \hat{I}(x,\omega^6) \end{aligned}$$

Then

$$\hat{I}(x,\omega) = I_1^+(x)w_1(\omega) + I_1^-(x)w_2(\omega) + \cdots + I_3^+(x)w_5(\omega) + I_3^-(x)w_6(\omega)$$

because of

$$w_j(\omega^i) = \delta_{ij}, \quad 1\le i,j\le 6.$$

By introducing $F_i := I_i^+ + I_i^-$ and $q_i := I_i^+ - I_i^-$, for $1\le i\le 3$, the six-flux method for the semidiscretization in ω leads to the boundary-value problem,

$$\begin{cases} -\dfrac{\partial}{\partial x_i}\left(\beta\dfrac{\partial F_i}{\partial x_i}\right) + KF_i - 2\sigma_s\displaystyle\sum_{\substack{j=1\\ j\neq i}}^{3} F_j = \frac{2a\sigma T^4}{\pi} \quad \text{in } \Omega, \quad 1\le i\le 3 \\ F_i + \dfrac{n_i}{|n_i|}\beta\dfrac{\partial F_i}{\partial x_i} = -\dfrac{1-\varepsilon_w}{\varepsilon_w}\left[\beta\displaystyle\sum_{i=1}^{3}\frac{\partial F_i}{\partial x_i}n_i\right] + 2\frac{\sigma T_w^4}{\pi} \quad \text{on } \Gamma, \quad 1\le i\le 3 \end{cases}$$

3.2.2 Finite elements

The algorithm proposed is the following:

Step 0. Input F_i^0, $0 \leq i \leq 3$

Step n+1. Given F_i^n, F_i^{n+1} are solution of the problems:

$$\int_\Omega \beta \frac{\partial F_i^{n+1}}{\partial x_i}\frac{\partial z_i}{\partial x_i}dx + \int_\Omega K F_i^{n+1} z_i dx + \int_\Gamma \frac{1+C_2C_3}{C_1} F_i^{n+1} z_i |n_i| d\Gamma - \int_\Gamma \frac{C_2}{C_1}(\sum_{\substack{j=1\\ j\neq i}}^{3} F_j^n |n_j|) z_i |n_i| d\Gamma -$$

$$- \int_\Gamma \frac{1}{C_1}\frac{2\sigma T_w^4}{\pi} z_i |n_i| d\Gamma - \int_\Omega 2\sigma_s s (\sum_{\substack{j=1\\ j\neq i}}^{3} F_j^n) z_i dx = \int_\Omega \frac{2a_g \sigma T^4}{\pi} z_i dx + \int_\Omega \frac{2a_s \sigma T_s^4}{\pi} z_i dx$$

where

$$C_1 = 1 + \frac{1-\varepsilon_w}{\varepsilon_w}\left(\sum_{j=1}^{3} |n_j|\right)$$

$$C_2 = \frac{1-\varepsilon_w}{\varepsilon_w}$$

$$C_3 = \sum_{\substack{j=1\\ j\neq i}}^{3} |n_j|$$

3.2.3 Finite Differences

We suppose that $\Omega = [0, l_x] \times [0, l_y] \times [0, l_z]$. Then the boundary condition above reads

$$\varepsilon_w F_i + \beta \frac{\partial F_i}{\partial x_i} n_i = \frac{2}{\pi}\varepsilon_w \sigma T_w^4 \quad \text{on } \Gamma.$$

The proposed algorithm is the following:

Step 0. Input F_i^0, $0 \leq i \leq 3$

Step n+1. Given F_i^n, we obtain F_1^{n+1} as the solution to the problems defined on lines parallel to the x axis

$$\begin{cases} -\dfrac{\partial}{\partial x}\left(\beta \dfrac{\partial F_1^{n+1}}{\partial x}\right) + K F_1^{n+1} = b^{1n} \ \text{ in } \Omega_x = [0, l_x] \times \{y_j\} \times \{z_l\}, \\ \beta \dfrac{\partial F_1^{n+1}}{\partial x} n_1 + \varepsilon_w F_1^{n+1} = \dfrac{2\sigma}{\pi}\varepsilon_w (T_w^n)^4 \ \text{ on } \Gamma_x = \{(0, y_j, z_l)\} \cup \{(l_x, y_j, z_l)\}, \end{cases}$$

with

$$b^{1n} = 2\sigma_s s \sum_{\substack{j=1\\ j\neq 1}}^{3} F_j^n + \frac{2a_g\sigma(T^n)^4}{\pi} + \frac{2a_s\sigma(T_s)^4}{\pi}.$$

This leads to the simple linear system

$$A\{F_1\} = S$$

where

$$A = \begin{pmatrix} d_p^1 & d_s^1 & & \\ d_s^1 & \ddots & \ddots & \\ & \ddots & \ddots & d_s^{n_x-1} \\ & & d_s^{n_x-1} & d_p^{n_x} \end{pmatrix} \qquad S = \begin{pmatrix} \frac{1}{2}h_1 b_1^1 + \frac{2\sigma}{\pi}\varepsilon_w (T_w(x_1, y_j, z_l))^4 \\ \vdots \\ \frac{1}{2}(h_{i-1} + h_i) b_i^1 \\ \vdots \\ \frac{1}{2}h_{n_x-1} b_{n_x}^1 + \frac{2\sigma}{\pi}\varepsilon_w (T_w(x_{n_x}, y_j, z_l))^4 \end{pmatrix}$$

$$d_p = \begin{pmatrix} \frac{1}{2}\frac{\beta_1 + \beta_2}{h_1} + \varepsilon_w + \frac{1}{2}h_1 K_1 \\ \vdots \\ \frac{1}{2}\frac{\beta_{i-1} + \beta_i}{h_{i-1}} + \frac{1}{2}\frac{\beta_i + \beta_{i+1}}{h_i} + \frac{1}{2}(h_{i-1} + h_i) K_i \\ \vdots \\ \frac{1}{2}\frac{\beta_{n_x-1} + \beta_{n_x}}{h_{n_x-1}} + \varepsilon_w + \frac{1}{2}h_{n_x-1} K_{n_x} \end{pmatrix} \qquad d_s = \begin{pmatrix} -\frac{1}{2}\frac{\beta_1 + \beta_2}{h_1} \\ \vdots \\ -\frac{1}{2}\frac{\beta_{n_x-1} + \beta_{n_x}}{h_{n_x-1}} \end{pmatrix}$$

$$F_1 = (F_{11}, \ldots, F_{1n_x})^T$$

and $F_{1i} = F_1^{n+1}(x_i, y_j, x_l), \;\; i = 1, \ldots, n_x$.

In a similar way, we proceed with lines parallel to the axis y and z, giving values of F_2^{n+1} and F_3^{n+1}, respectively.

3.3 Advection-diffusion equations

The advection-diffusion-reaction equations of the gas-phase model are of the general form,

$$\rho \frac{Du(x,t)}{Dt} - \nabla \cdot (\rho(x,t)\mathcal{D}(x)\nabla u(x,t)) + c(x,t)u(x,t) = f(x,t).$$

More specifically, the energy and mass conservation equations are of this type. In order to solve them we use a second order semi-Lagrange-Galerkin scheme. We discretize the convective term using the formula

$$\frac{Du}{Dt} = \frac{\partial u}{\partial t} + \mathbf{v} \cdot \nabla u \approx \frac{1}{2\Delta t}\left(3u^{n+1} - 4u^n \circ \chi^n + u^{n-1} \circ \chi^{n-1}\right),$$

where

$$\chi^n(x) = \chi(x, t^{n+1}; t^n)$$

is the position at time $t = t^n$ of the fluid particle that is at point x at time t^{n+1} and that moves with velocity $\mathbf{v}$. The characteristic curves $\chi(x, s; t)$ are the unique solution of the ODE

$$\begin{aligned} &\frac{d\chi(x,s;t)}{dt} = \mathbf{v}(\chi(x,s;t), t), \quad s, t \in [0, T] \\ &\chi(x, s; s) = x. \end{aligned}$$

To solve this ODE we can use a fourth-order Runge-Kutta method or a third-order fixed point method with the operator $T : \Omega \to \Omega$ defined by

$$T = \Delta t \left(1.5\mathbf{v}^n - 0.5\mathbf{v}^{n-1}\right)$$

that satisfies $Ty = y$ with

$$y = x - \chi(x, t^{n+1}; t^n).$$

The latter makes possible to adapt the time step.

3.4 Algorithm for the solid phase model

In order to solve the combustion model introduced in the previous sections, we have designed an algorithm which distinguishes, at each time step, the combustion stage in which the particle is. In Figure 3.4 we can see a scheme of this algorithm that we apply to each single particle.

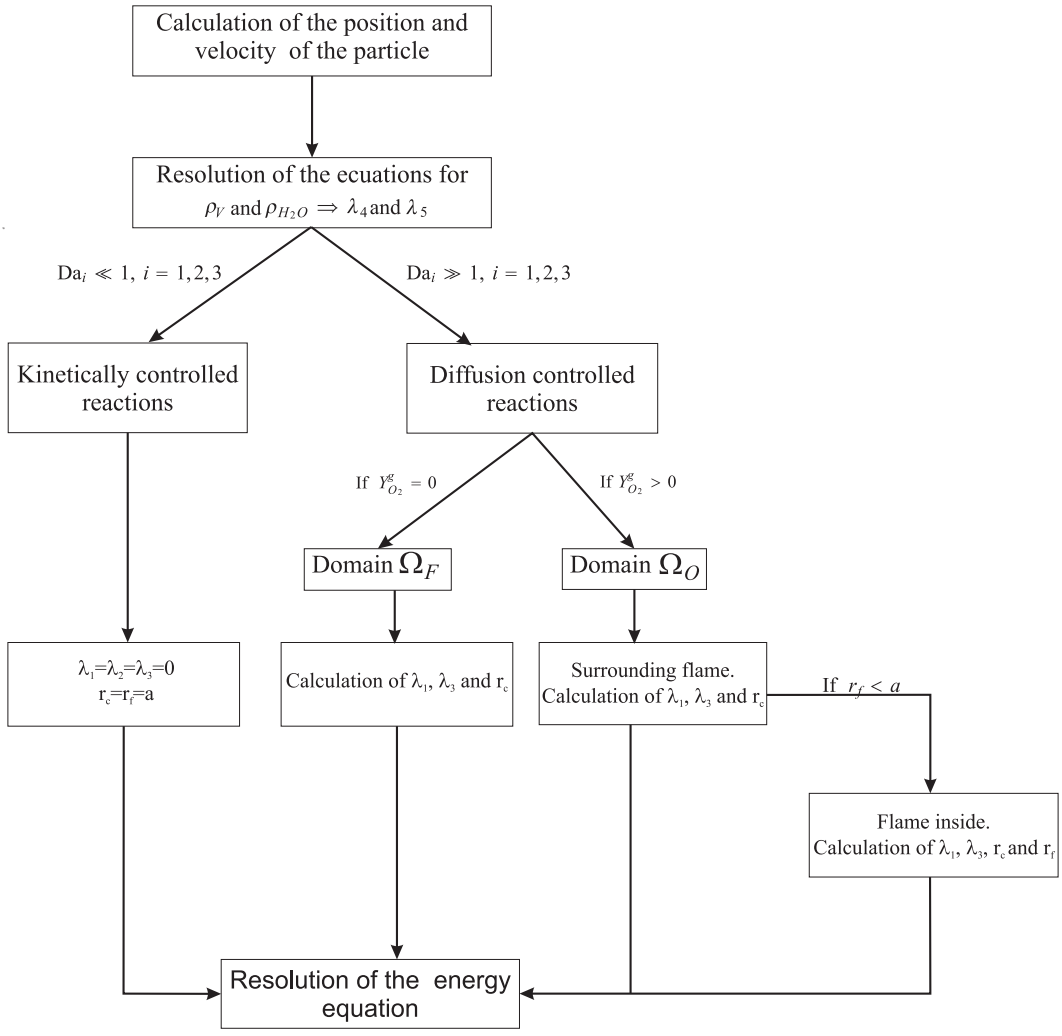

Figure 8.— Algorithm for solving the combustion model

4 Numerical Results

4.1 Analysis of numerical diffusion

Results of the study of the numerical diffusion when solving a convection-diffusion equation with the finite element method introduced in the previous section can be seen in Figure 4.1. They could be compared, for instance, with those of [5].

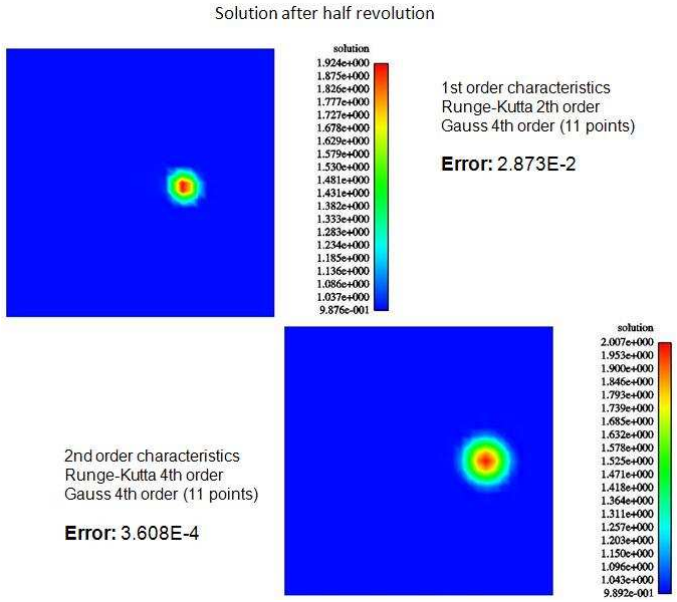

Figure 9.— Comparison of results for a benchmark 3D test

4.2 A coal flame simulation

A detailed study of the structure of a turbulent pulverized coal flame has been done in Hwang *et al* [3, 4].

Our purpose will be to do a full numerical simulation of the turbulent pulverized coal burner, used in these articles (see Figure 10).

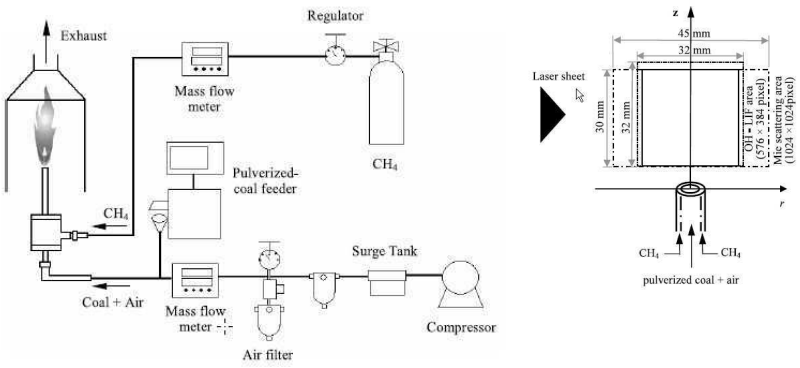

Figure 10.— Scheme of the experiment

In this study, methane is supplied to ignite the two-phase jet because the coal injection rate is very small and flame stabilization is impossible for a pure pulverized coal flame. The methane flow rate is the minimum amount needed to form a stable flame. The experiment is designed as follows: first the air is supplied to the main burner port and the methane to the annular slit burner. Next the gas flame due to the air and the methane is formed, and finally, when the methane diffusion flame becomes stable, the pulverized coal particles are dropped.

In order to make a numerical simulation of this experiment we proceed to the following steps:

1. We make a simulation with Fluent of the first stage of the experiment, until the methane flame is stable. Figure 11 shows the geometrical domain for the CFD simulation. The data corresponding to flows are: through the coal-air inlet 1.8×10^{-4} kg/s of air and 1.49×10^{-4} kg/s of coal are introduced whereas 1.67×10^{-5} kg/s of gas enters through the gas inlet.

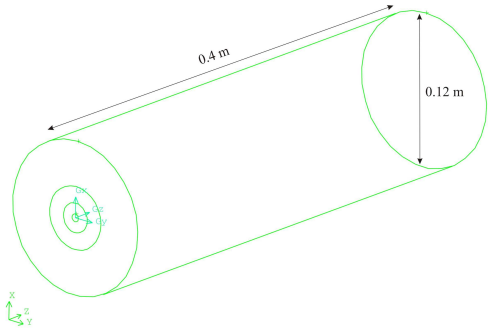

Figure 11.— Geometry of the burner

2. With the results of the gas phase obtained from the Fluent simulation we solve our combustion model.

3. We solve the combustion model with Fluent (namely Discrete Phase Model) starting at the same initial data.

4. We compare results provided by both methods.

Figures 12 and 13 show the homogenized sources of total mass and O_2, respectively, obtained with both models.

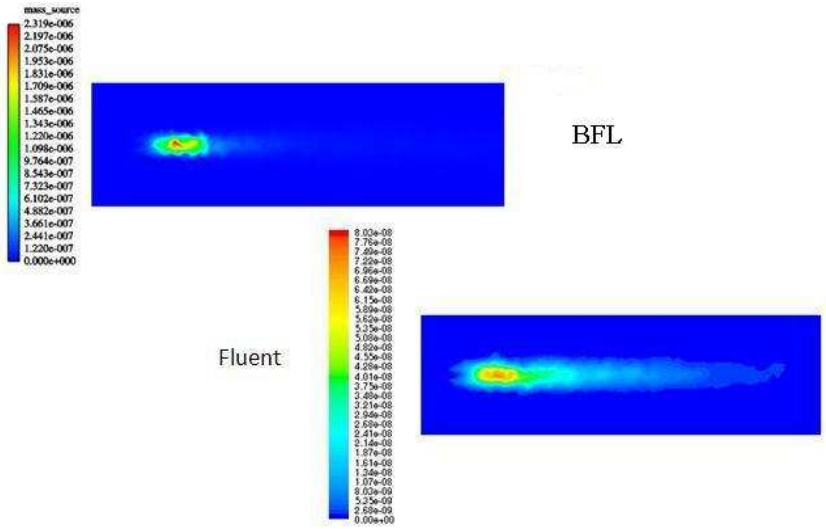

Figure 12.— Source of mass (f^{m})

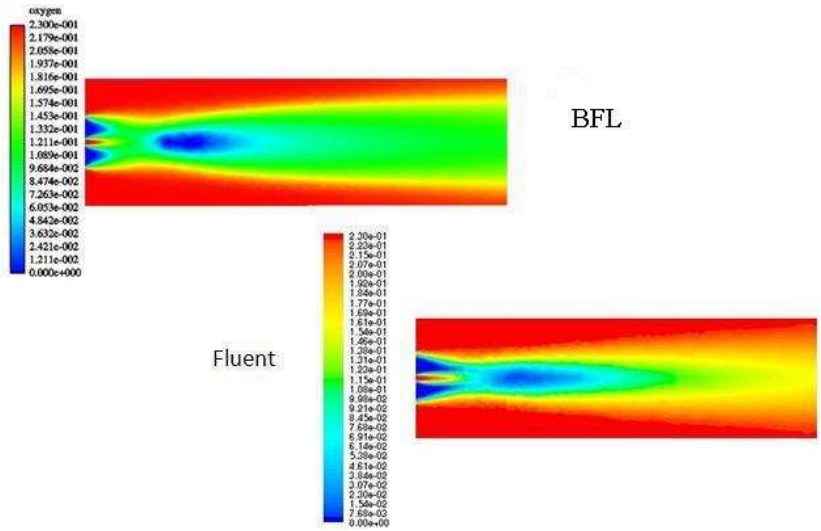

Figure 13.— Source of O_2 ($f^{\mathrm{m}}_{O_2}$)

Furthermore, with respect to unburned coal we have obtained the following results from the two different models:

- Fluent:
  Volume integral of mass source: 6.34664×10^{-5} kg/s
  Mass of released volatiles: 94.54 %
  Mass of gasified char: 50.50 %

- BFL:
  Volume integral of mass source: 7.55143×10^{-5} kg/s
  Mass of released volatiles: 98.31 %
  Mass of gasified char: 44.53 %

5 Conclusions

We have proposed a mathematical model for a pulverized coal furnace and subsequently numerical methods for solving it. For validation purposes, we have simulated an experiment involving the combustion of pulverized coal particles in a cylindrical domain. Results obtained have been compared with those given by Fluent.

Acknowledgment

Part of this work was supported by Ministerio de Educación y Ciencia through project ENE2005-09190-C04-01: "Investigación Aplicada en Conversión Limpia de Combustibles Fósiles (CLCF)"

References

[1] K. Annamalai and W. Ryan. Interactive processes in gasification and combustion. II Isolated carbon, coal and porous char particles. *Progr. Energy Combust. Sci.*, 19:383–446 (1993).

[2] A. Bermúdez and J.L. Ferrín and A. Liñán. The modelling of the generation of volatiles, H_2 and CO, and their simultaneous diffusion controlled oxidation, in pulverised coal furnaces. *Combustion Theory and Modelling*, 11:949–976 (2007).

[3] S-M. Hwang, R. Kurose, F. Akamatsu, H. Tsuji, H. Makino and M. Katsuki. Observation of detailed structure of turbulent pulverized-coal flame by optical measurement (Part 1, time-averaged measurement of behavior of pulverised-coal particles and flame structure). *JSME International Journal*, 49(4):1316–1327, 2006.

[4] S-M. Hwang, R. Kurose, F. Akamatsu, H. Tsuji, H. Makino and M. Katsuki. Observation of detailed structure of turbulent pulverized-coal flame by optical measurement (Part 2, instantaneous two-dimensional measurement of combustion reaction zone and pulverised coal particles). *JSME International Journal*, 49(4):1328–1335, 2006.

[5] M.R. Kaazempur-M. and C.R. Ethier. An efficient characteristic Galerkin scheme for the advection equation in 3-D. *Comput. Methods Appl. Mech. Engrg.*, 191:5345-5363, 2002.

[6] J.M. Macinnes and F. V. Bracco. Stochastic particle dispersion modeling and the tracer-particle limit *Phys. Fluids*, 12:2809–2824 (1992).

[7] F.A. Williams. *Combustion Theory.* The Benjamin/Cummings Publ. Co., Inc, Menlo Park, 1985.

[8] A.D. Gosman and E. Ioannides. Aspects of computer simulation of liquid-fueled combustors. *J. Energy*, 7(6):482–490, 1983.

[9] Q. Zhou and M.A. Leschziner. A time-correlated stochastic model for particle dispersion in anisotropic turbulence. *8th Turbulent Shear Flows Symposium.*, Munich, 1991.